



Universiteit  
Leiden  
The Netherlands

## **$\gamma\delta$ T cells are effectors of immunotherapy in cancers with HLA class I defects**

Vries, N.L. de; Haar, J. van de; Veninga, V.; Chalabi, M.; Ijsselsteijn, M.E.; Ploeg, M. van der; ... ; Voest, E.E.

### **Citation**

Vries, N. L. de, Haar, J. van de, Veninga, V., Chalabi, M., Ijsselsteijn, M. E., Ploeg, M. van der, ... Voest, E. E. (2023).  $\gamma\delta$  T cells are effectors of immunotherapy in cancers with HLA class I defects. *Nature*, 613(7945), 743-750. doi:10.1038/s41586-022-05593-1

Version: Publisher's Version

License: [Creative Commons CC BY 4.0 license](https://creativecommons.org/licenses/by/4.0/)

Downloaded from: <https://hdl.handle.net/1887/3714017>

**Note:** To cite this publication please use the final published version (if applicable).

# $\gamma\delta$ T cells are effectors of immunotherapy in cancers with HLA class I defects

<https://doi.org/10.1038/s41586-022-05593-1>

Received: 16 July 2021

Accepted: 24 November 2022

Published online: 11 January 2023

Open access

 Check for updates

Natasja L. de Vries<sup>1,2,13</sup>, Joris van de Haar<sup>3,4,5,13</sup>, Vivien Veninga<sup>3,4,13</sup>, Myriam Chalabi<sup>3,6,7,13</sup>, Marieke E. Ijsselsteijn<sup>1</sup>, Manon van der Ploeg<sup>1</sup>, Jitske van den Bulk<sup>1</sup>, Dina Ruano<sup>1</sup>, Jose G. van den Berg<sup>8</sup>, John B. Haanen<sup>3,7</sup>, Laurien J. Zeveijjn<sup>3,4</sup>, Birgit S. Geurts<sup>3,4</sup>, Gijs F. de Wit<sup>3,4</sup>, Thomas W. Battaglia<sup>3,4</sup>, Hans Gelderblom<sup>9</sup>, Henk M. W. Verheul<sup>10</sup>, Ton N. Schumacher<sup>3,4,11</sup>, Lodewyk F. A. Wessels<sup>4,5,12</sup>, Frits Koning<sup>2,14</sup>, Noel F. C. C. de Miranda<sup>1,14</sup>✉ & Emile E. Voest<sup>3,4,14</sup>✉

DNA mismatch repair-deficient (MMR-d) cancers present an abundance of neoantigens that is thought to explain their exceptional responsiveness to immune checkpoint blockade (ICB)<sup>1,2</sup>. Here, in contrast to other cancer types<sup>3–5</sup>, we observed that 20 out of 21 (95%) MMR-d cancers with genomic inactivation of  $\beta 2$ -microglobulin (encoded by *B2M*) retained responsiveness to ICB, suggesting the involvement of immune effector cells other than CD8<sup>+</sup> T cells in this context. We next identified a strong association between *B2M* inactivation and increased infiltration by  $\gamma\delta$  T cells in MMR-d cancers. These  $\gamma\delta$  T cells mainly comprised the V $\delta$ 1 and V $\delta$ 3 subsets, and expressed high levels of PD-1, other activation markers, including cytotoxic molecules, and a broad repertoire of killer-cell immunoglobulin-like receptors. In vitro, PD-1<sup>+</sup>  $\gamma\delta$  T cells that were isolated from MMR-d colon cancers exhibited enhanced reactivity to human leukocyte antigen (HLA)-class-I-negative MMR-d colon cancer cell lines and *B2M*-knockout patient-derived tumour organoids compared with antigen-presentation-proficient cells. By comparing paired tumour samples from patients with MMR-d colon cancer that were obtained before and after dual PD-1 and CTLA-4 blockade, we found that immune checkpoint blockade substantially increased the frequency of  $\gamma\delta$  T cells in *B2M*-deficient cancers. Taken together, these data indicate that  $\gamma\delta$  T cells contribute to the response to immune checkpoint blockade in patients with HLA-class-I-negative MMR-d colon cancers, and underline the potential of  $\gamma\delta$  T cells in cancer immunotherapy.

ICB targeting the PD-1–PD-L1 and/or CTLA-4 axes provides durable clinical benefits to patients who have cancers with MMR-d and high microsatellite instability<sup>6–9</sup>. The exceptional responses of cancers with MMR-d and high microsatellite instability to ICB is thought to be explained by their substantial burden of putative neoantigens, which originate from the extensive accumulation of mutations in their genomes<sup>1,2</sup>. This is consistent with the current view that PD-1 blockade mainly boosts endogenous antitumour immunity driven by CD8<sup>+</sup> T cells, which recognize HLA-class-I-bound neoepitopes on cancer cells<sup>10–12</sup>. However, MMR-d colon cancers frequently lose HLA-class-I-mediated antigen presentation due to silencing of HLA class I genes, inactivating mutations in  $\beta 2$ -microglobulin (encoded by *B2M*) or other defects in the antigen processing machinery<sup>13–16</sup>, which can render these tumours resistant to CD8<sup>+</sup> T-cell-mediated immunity<sup>3–5,17</sup>. Notably, early evidence has indicated that *B2M*-deficient, MMR-d cancers can obtain durable

responses to PD-1 blockade<sup>18</sup>, suggesting that immune cell subsets other than CD8<sup>+</sup> T cells contribute to these responses.

HLA-class-I-unrestricted immune cell subsets, which have the ability to kill tumour cells, include natural killer (NK) cells and  $\gamma\delta$  T cells.  $\gamma\delta$  T cells share many characteristics with their  $\alpha\beta$  T cell counterpart, such as cytotoxic effector functions, but express a distinct TCR that is composed of a  $\gamma$  and a  $\delta$  chain. Different subsets of  $\gamma\delta$  T cells are defined by their TCR  $\delta$  chain use, of which those expressing V $\delta$ 1 and V $\delta$ 3 are primarily ‘tissue-resident’ at mucosal sites, whereas those expressing V $\delta$ 2 are mainly found in blood<sup>19</sup>. Both adaptive and innate mechanisms of activation—for example, through stimulation of their  $\gamma\delta$  TCR or innate receptors such as NKG2D, DNAM-1, NKp30 or NKp44—have been described for  $\gamma\delta$  T cells<sup>20</sup>. Killer-cell immunoglobulin-like receptors (KIRs) are expressed by  $\gamma\delta$  T cells and regulate their activity depending on HLA class I expression in target cells<sup>21</sup>. Furthermore,  $\gamma\delta$  T cells

<sup>1</sup>Department of Pathology, Leiden University Medical Center, Leiden, The Netherlands. <sup>2</sup>Department of Immunology, Leiden University Medical Center, Leiden, The Netherlands. <sup>3</sup>Department of Molecular Oncology and Immunology, Netherlands Cancer Institute, Amsterdam, The Netherlands. <sup>4</sup>Oncode Institute, Utrecht, The Netherlands. <sup>5</sup>Division of Molecular Carcinogenesis, Netherlands Cancer Institute, Amsterdam, The Netherlands. <sup>6</sup>Gastrointestinal Oncology, Netherlands Cancer Institute, Amsterdam, The Netherlands. <sup>7</sup>Medical Oncology, Netherlands Cancer Institute, Amsterdam, The Netherlands. <sup>8</sup>Department of Pathology, Netherlands Cancer Institute, Amsterdam, The Netherlands. <sup>9</sup>Department of Medical Oncology, Leiden University Medical Center, Leiden, The Netherlands. <sup>10</sup>Department of Medical Oncology, Erasmus MC, Rotterdam, The Netherlands. <sup>11</sup>Department of Hematology, Leiden University Medical Center, Leiden, The Netherlands. <sup>12</sup>Faculty of EEMCS, Delft University of Technology, Delft, The Netherlands. <sup>13</sup>These authors contributed equally: Natasja L. de Vries, Joris van de Haar, Vivien Veninga, Myriam Chalabi. <sup>14</sup>These authors jointly supervised this work: Frits Koning, Noel F. C. C. de Miranda, Emile E. Voest. ✉e-mail: n.f.de\_miranda@lumc.nl; e.voest@nki.nl

were found to express high levels of PD-1 in MMR-d colorectal cancers (CRCs)<sup>22</sup>, suggesting that these cells may be targeted by PD-1 blockade.

Here, we applied a combination of transcriptomic and imaging approaches for an in-depth analysis of ICB-naïve and ICB-treated MMR-d colon cancers, as well as in vitro functional assays, and found evidence indicating that  $\gamma\delta$  T cells mediate responses to HLA-class-I-negative MMR-d tumours during treatment with ICB.

### ICB is effective in $B2M^{MUT}$ MMR-d cancers

We evaluated responses to PD-1 blockade therapy in a cohort of 71 patients with MMR-d cancers from various anatomical sites treated in the Drug Rediscovery Protocol (DRUP)<sup>23</sup> in relation to their  $B2M$  status (Fig. 1a, Extended Data Fig. 1a–c and Supplementary Table 1). A clinical benefit (CB; defined as at least 4 months of disease control; the primary outcome of the DRUP) was observed in 20 out of 21 (95%) of patients with tumours with mutant or deleted  $B2M$  ( $B2M^{MUT}$ ) tumours versus 31 out of 50 (62%) of patients with tumours with wild-type  $B2M$  ( $B2M^{WT}$ ) (two-sided Fisher's exact test,  $P = 0.0038$ ; logistic regression,  $P = 0.022$  and  $P = 0.027$ , adjusted for tumour mutational burden (TMB), and TMB plus tumour type, respectively; Fig. 1b). Among patients with  $B2M^{MUT}$  tumours, 3 out of 21 (14%) individuals experienced a complete response (according to RECIST1.1 criteria), 12 (57%) experienced a partial response, 5 (24%) experienced a durable stable disease and 1 (4.8%) experienced progressive disease as the best overall response. All 44  $B2M$  alterations across 21 patients were clonal (Methods), consistent with previous observations in MMR-d cancers<sup>18</sup>. A total of 13 out of 21 (62%) patients with  $B2M^{MUT}$  tumours had biallelic  $B2M$  alterations, 4 (19%) had potentially biallelic alterations and 4 (19%) had non-biallelic alterations (Fig. 1c and Methods). Non-biallelic alterations have also been associated with complete loss of  $B2M$  protein expression in MMR-d tumours<sup>18</sup>. Thus,  $B2M$  alterations are associated with a high clinical benefit rate of PD-1 blockade in patients with MMR-d cancers.

### V $\delta$ 1 and V $\delta$ 3 TCRs are overexpressed in $B2M^{MUT}$ cancers

To gain insights into the immune cell subsets that are involved in immune responses to HLA-class-I-negative MMR-d cancers, we used data of The Cancer Genome Atlas (TCGA) and studied the transcriptomic changes associated with the genomic loss of  $B2M$  in three cohorts of individuals with MMR-d cancer in colon adenocarcinoma (COAD;  $n = 50$  ( $B2M^{WT}$ ),  $n = 7$  ( $B2M^{MUT}$ )), stomach adenocarcinoma (STAD;  $n = 48$  ( $B2M^{WT}$ ) and  $n = 12$  ( $B2M^{MUT}$ )), and endometrium carcinoma (UCEC;  $n = 118$  ( $B2M^{WT}$ ) and  $n = 4$  ( $B2M^{MUT}$ )). We found that  $B2M$  was among the most significantly downregulated genes in  $B2M^{MUT}$  cancers (two-sided limma-voom-based regression,  $P = 3.5 \times 10^{-4}$ , Benjamini–Hochberg false-discovery rate (FDR)-adjusted  $P = 0.12$ , adjusted for tumour type; Fig. 1d). Genes encoding components of the HLA class I antigen presentation machinery other than  $B2M$  were highly upregulated in  $B2M^{MUT}$  tumours, which may reflect reduced evolutionary pressure on somatic inactivation of these genes in the  $B2M^{MUT}$  context<sup>18</sup> (Fig. 1d). Notably, we found  $TRDV1$  and  $TRDV3$ , which encode the variable regions of the  $\delta 1$  and  $\delta 3$  chains of the  $\gamma\delta$  T cell receptor (TCR), among the most significantly upregulated loci in  $B2M^{MUT}$  tumours ( $TRDV1$ , two-sided limma-voom-based regression, FDR-adjusted  $P = 0.00090$ , adjusted for tumour type;  $TRDV3$ , two-sided limma-voom-based regression, FDR-adjusted  $P = 0.0015$ , adjusted for tumour type; Fig. 1d), regardless of the allelic status of the  $B2M$  alteration (Extended Data Fig. 1d). Consistent with this, the expression levels of  $TRDV1$  and  $TRDV3$  were higher in  $B2M^{MUT}$  compared with in  $B2M^{WT}$  MMR-d cancers (two-sided Wilcoxon rank-sum test,  $P = 6.5 \times 10^{-8}$  for all of the cohorts combined; two-sided linear regression,  $P = 4.7 \times 10^{-6}$ , adjusted for tumour type; Fig. 1d–f). Moreover,  $B2M^{MUT}$  tumours showed overexpression of multiple KIRs

(Fig. 1d), which clustered together with  $TRDV1$  and  $TRDV3$  on the basis of hierarchical clustering (Extended Data Fig. 1e). The expression level of different KIRs (Supplementary Table 2) was higher in  $B2M^{MUT}$  tumours compared with in  $B2M^{WT}$  MMR-d tumours (two-sided Wilcoxon rank-sum test,  $P = 4.4 \times 10^{-6}$  for all cohorts combined; two-sided linear regression,  $P = 4.7 \times 10^{-5}$ , adjusted for tumour type; Fig. 1d–f). Together, these results suggest that ICB-naïve  $B2M^{MUT}$  MMR-d cancers show increased levels of V $\delta$ 1 and V $\delta$ 3 T cells as well as increased numbers of these or other immune cells expressing KIRs—a potential mechanism of recognition of HLA class I loss.

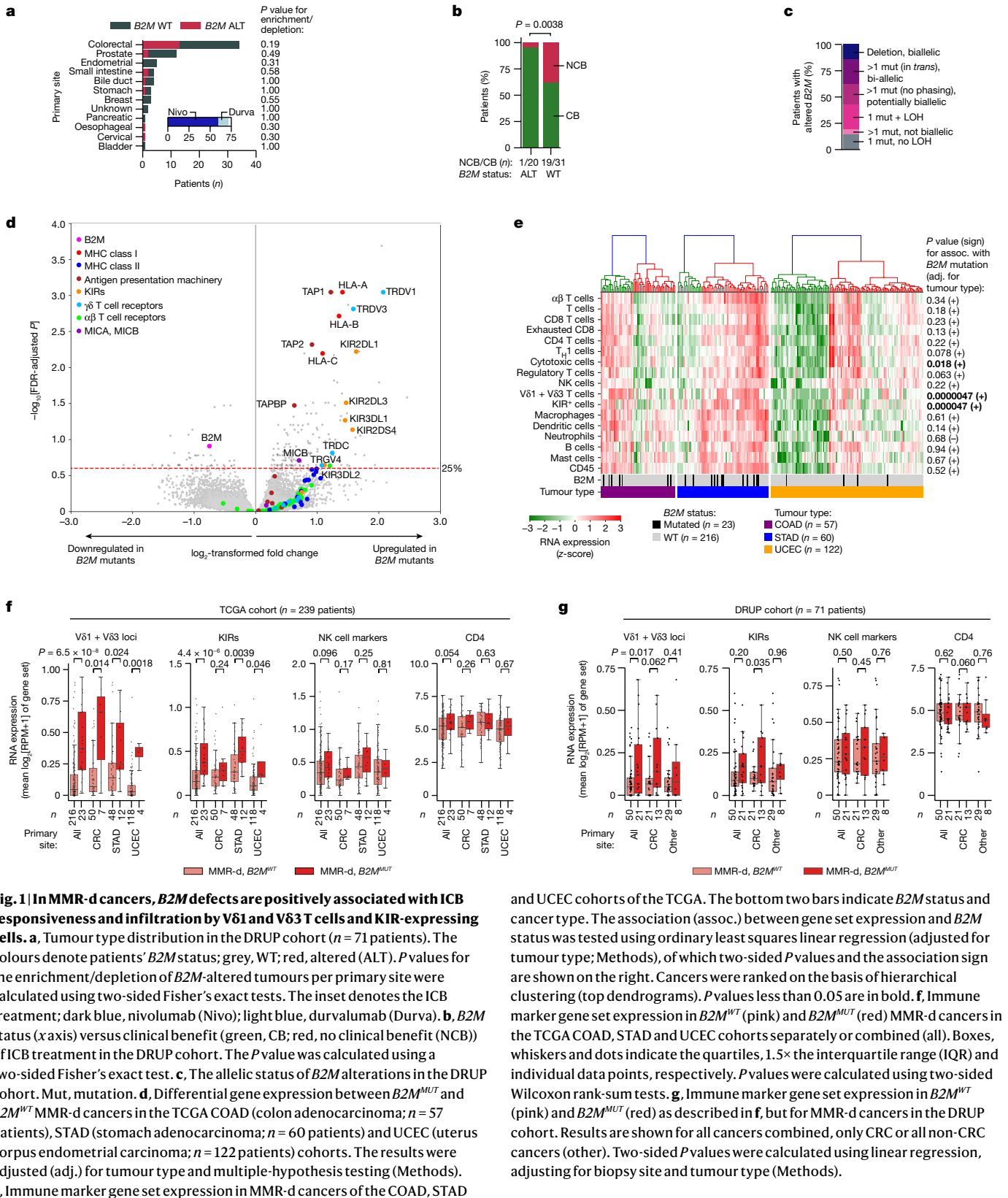
We used marker gene sets (modified from ref. <sup>24</sup>; Methods and Supplementary Table 2) to estimate the abundance of a broad set of other immune cell types on the basis of the RNA expression data of the TCGA cohorts. Hierarchical clustering identified a high- and a low-infiltrated cluster in each of the three tumour types (Fig. 1e). Compared with the V $\delta$ 1 and V $\delta$ 3 T cell and KIR gene sets, the other marker gene sets showed no or only weak association between expression level and  $B2M$  status, indicating that our findings were not solely driven by a generally more inflamed state of  $B2M^{MUT}$  tumours (Fig. 1e, and Extended Data Fig. 1f).

We next revisited the DRUP cohort and specifically applied the marker gene sets to RNA expression data. Despite the low patient numbers and high heterogeneity regarding tumour types and biopsy locations of this cohort, we confirmed increased  $TRDV1$  and  $TRDV3$  expression in  $B2M^{MUT}$  tumours pan-cancer (two-sided linear regression,  $P = 0.017$ , adjusted for tumour type and biopsy site; Fig. 1g, Extended Data Fig. 1g and Methods). KIR expression was significantly associated with  $B2M$  status only in CRC (Fig. 1g). Across mismatch repair-proficient (MMR-p) metastatic cancers in the Hartwig database<sup>25</sup>, 36 out of 2,256 (1.6%) cancers had a clonal  $B2M$  alteration, which was frequently accompanied by loss of heterozygosity (LOH) (Extended Data Fig. 1h and Supplementary Table 3). Although rare,  $B2M$  alterations were also significantly associated with increased expression of  $TRDV1/TRDV3$  loci in this context (two-sided linear regression,  $P = 2.2 \times 10^{-17}$ , adjusted for tumour type; Extended Data Fig. 1i and Methods). Taken together,  $B2M$  defects are positively associated with clinical benefits of ICB treatment, as well as infiltration by V $\delta$ 1 and V $\delta$ 3 T cells and expression of KIRs.

### V $\delta$ 1 and V $\delta$ 3 T cells are activated in MMR-d CRC

To investigate which  $\gamma\delta$  T cell subsets are present in MMR-d colon cancers and to determine their functional characteristics, we performed single-cell RNA-sequencing (scRNA-seq) analysis of  $\gamma\delta$  T cells isolated from five MMR-d colon cancers (Extended Data Figs. 2 and 3 and Supplementary Table 4). Three distinct V $\delta$  subsets were identified (Fig. 2a)—V $\delta$ 1 T cells were the most prevalent (43% of  $\gamma\delta$  T cells), followed by V $\delta$ 2 (19%) and V $\delta$ 3 T cells (11%) (Fig. 2b).  $PDCDI$  (encoding PD-1) was predominantly expressed by V $\delta$ 1 and V $\delta$ 3 T cells, whereas V $\delta$ 1 cells expressed high levels of genes that encode activation markers such as CD39 ( $ENTPDI$ ) and CD38 (Fig. 2c and Extended Data Fig. 2b). Furthermore, proliferating  $\gamma\delta$  T cells (expressing  $MKI67$ ) were especially observed in the V $\delta$ 1 and V $\delta$ 3 subsets (Fig. 2c). Other distinguishing features of the V $\delta$ 1 and V $\delta$ 3 T cell subsets included the expression of genes encoding activating receptors Nkp46 (encoded by  $NCR1$ ), NKG2C (encoded by  $KLRC2$ ) and NKG2D (encoded by  $KLRI1$ ) (Fig. 2c). Notably, the expression of several KIRs was also higher in the V $\delta$ 1 and V $\delta$ 3 subsets as compared to V $\delta$ 2 T cells (Fig. 2c). Almost all  $\gamma\delta$  T cells displayed expression of the genes encoding granzyme B ( $GZMB$ ), perforin ( $PRFI$ ) and granulysin ( $GPLY$ ) (Fig. 2c). Together, these data support a role for  $\gamma\delta$  T cells in mediating natural cytotoxic antitumour responses in HLA-class-I-negative MMR-d colon cancers.

Next, we applied imaging mass cytometry (IMC) analysis to a cohort of 17 individuals with ICB-naïve MMR-d colon cancers (Supplementary Table 4). High levels of  $\gamma\delta$  T cell infiltration were observed in cancers with  $B2M$  defects as compared to  $B2M$ -proficient cancers, albeit this



difference was not significant (Fig. 2d). The levels of other immune cells, including NK cells,  $CD4^+$  T cells and  $CD8^+$  T cells, were similar between  $B2M$ -deficient and  $B2M$ -proficient tumours (Fig. 2d). In  $B2M$ -deficient cancers,  $\gamma\delta$  T cells showed frequent intraepithelial localization and expression of CD103 (tissue-residency), CD39 (activation), granzyme

B (cytotoxicity) and Ki-67 (proliferation), as well as PD-1 (Fig. 2d–f and Extended Data Fig. 2c), consistent with the scRNA-seq data. Notably,  $\gamma\delta$  T cells in  $B2M$ -deficient cancers showed co-expression of CD103 and CD39 (Extended Data Fig. 2d), which has been reported to identify tumour-reactive  $CD8^+$   $\alpha\beta$  T cells in a variety of cancers<sup>26</sup>.

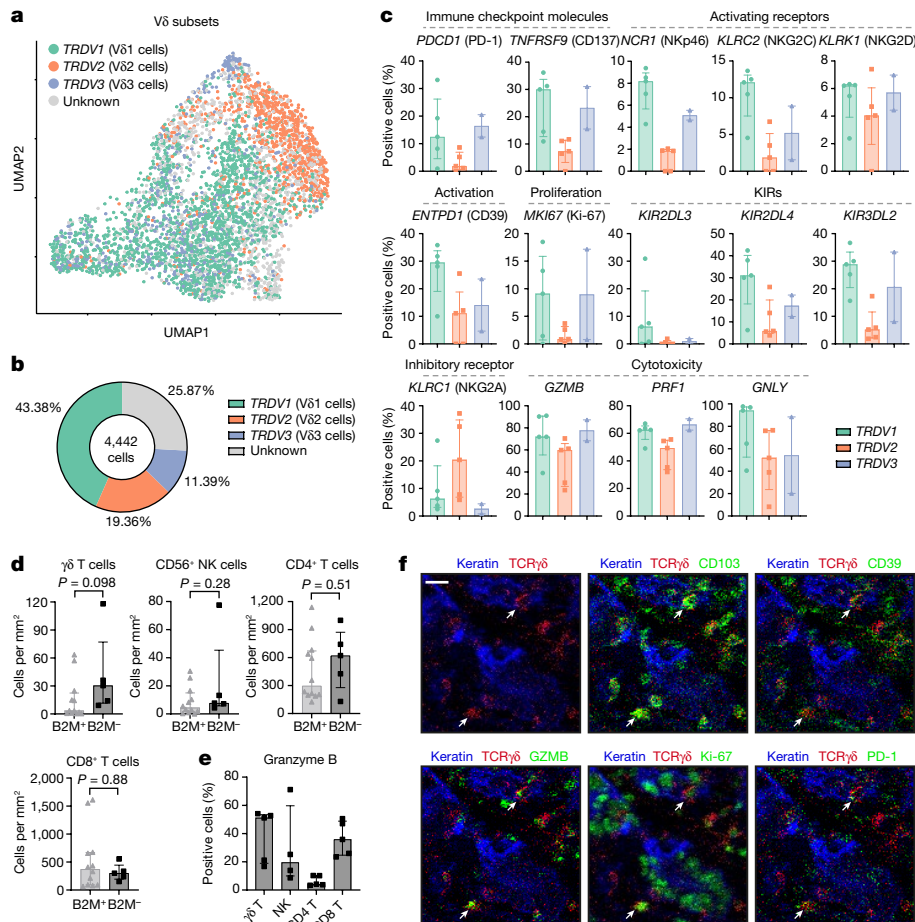


**Fig. 2 | Tumour-infiltrating Vδ1 and Vδ3 T cell subsets display hallmarks of cytotoxic activity in MMR-d colon cancers.** **a**, UMAP embedding showing the clustering of  $\gamma\delta$  T cells ( $n = 4,442$ ) isolated from MMR-d colon cancers ( $n = 5$ ) analysed using scRNA-seq. The colours represent the TCR Vδ chain usage. The functionally distinct  $\gamma\delta$  T cell clusters are shown in Extended Data Fig. 3. Dots represent single cells. **b**, The frequencies of TCR Vδ chain use of the  $\gamma\delta$  T cells ( $n = 4,442$ ) analysed using scRNA-seq as a percentage of total  $\gamma\delta$  T cells. **c**, The frequencies of positive cells for selected genes across Vδ1 ( $n = 1,927$ ), Vδ2 ( $n = 860$ ) and Vδ3 ( $n = 506$ ) cells as the percentage of total  $\gamma\delta$  T cells from each MMR-d colon tumour ( $n = 5$ ) analysed using scRNA-seq. Vδ3 cells were present in two out of five colon cancers. Data are median  $\pm$  IQR, with individual samples

(dots). **d**, The frequencies of  $\gamma\delta$  T cells, CD56<sup>+</sup> NK cells, CD4<sup>+</sup> T cells and CD8<sup>+</sup> T cells in treatment-naive B2M<sup>+</sup> ( $n = 12$ ) and B2M<sup>-</sup> ( $n = 5$ ) MMR-d colon cancers. Data are median  $\pm$  IQR, with individual samples (dots). *P* values were calculated using two-sided Wilcoxon rank-sum tests. **e**, The frequencies of granzyme-B-positive  $\gamma\delta$  T cells, CD56<sup>+</sup> NK cells, CD4<sup>+</sup> T cells and CD8<sup>+</sup> T cells in treatment-naive B2M<sup>-</sup> ( $n = 5$ ) MMR-d colon cancers. CD56<sup>+</sup> NK cells were present in four out of five B2M<sup>-</sup> cancer samples. Data are median  $\pm$  IQR, with individual samples (dots). **f**, Representative images of the detection of tissue-resident (CD103<sup>+</sup>), activated (CD39<sup>+</sup>), cytotoxic (granzyme B<sup>+</sup>), proliferating (Ki-67<sup>+</sup>) and PD-1<sup>+</sup>  $\gamma\delta$  T cells (white arrows) by IHC analysis of a treatment-naive MMR-d colon cancer with B2M defects. Scale bar, 20  $\mu$ m.

### PD-1<sup>+</sup> Vδ1 and Vδ3 T cells kill HLA-class-I<sup>-</sup> CRC cells

We next sought to determine whether tumour-infiltrating  $\gamma\delta$  T cells can recognize and kill CRC cells. We isolated and expanded PD-1<sup>-</sup> and PD-1<sup>+</sup>  $\gamma\delta$  T cells from five MMR-d colon cancers (Extended Data Fig. 4a–c and Supplementary Table 4). Consistent with the scRNA-seq data, expanded PD-1<sup>+</sup>  $\gamma\delta$  T cell populations lacked Vδ2<sup>+</sup> cells and comprised the Vδ1<sup>+</sup> or Vδ3<sup>+</sup> subsets, whereas the PD-1<sup>-</sup> fractions contained Vδ2<sup>+</sup> or a mixture of Vδ1<sup>+</sup>, Vδ2<sup>+</sup> and Vδ3<sup>+</sup> populations (Fig. 3a and Extended Data Fig. 4d). Detailed immunophenotyping of the expanded  $\gamma\delta$  T cells (Fig. 3a and Extended Data Fig. 5a) showed that all of the subsets expressed the activating receptor NKG2D, whereas the surface expression of natural cytotoxicity receptors (NCRs) and KIRs was most frequent on PD-1<sup>+</sup>  $\gamma\delta$  T cells (Vδ1 or Vδ3<sup>+</sup>), consistent with the scRNA-seq results of unexpanded populations.

We measured the reactivity of the expanded  $\gamma\delta$  T cell populations to HLA-class-I-negative and HLA-class-I-positive cancer cell lines (Fig. 3b and Extended Data Fig. 4b). After co-culture with the different cancer cell lines, reactivity (assessed by expression of activation markers and

secretion of IFN $\gamma$ ) was largely restricted to PD-1<sup>+</sup>  $\gamma\delta$  T cells (Vδ1 or Vδ3<sup>+</sup>), whereas activation of PD-1<sup>-</sup>  $\gamma\delta$  T cells (Vδ2<sup>+</sup>) was generally not detected (Fig. 3c and Extended Data Fig. 4). PD-1<sup>+</sup>  $\gamma\delta$  T cell (Vδ1 or Vδ3<sup>+</sup>) reactivity was variable and was observed against both HLA-class-I-negative and HLA-class-I-positive cell lines (Fig. 3c and Extended Data Fig. 4). To quantify and visualize the differences in the killing of CRC cell lines by PD-1<sup>+</sup> and PD-1<sup>-</sup>  $\gamma\delta$  T cells, we co-cultured the  $\gamma\delta$  T cell populations with three CRC cell lines (HCT-15, LoVo, HT-29) in the presence of a fluorescent cleaved-caspase-3/7 reporter to measure cancer cell apoptosis over time (Fig. 3d,e). We found pronounced cancer cell apoptosis after co-culture with PD-1<sup>+</sup>  $\gamma\delta$  T cells (Vδ1 or Vδ3<sup>+</sup>) compared with PD-1<sup>-</sup> cells; cancer cell death was more pronounced in HLA-class-I-negative HCT-15 cells (Fig. 3e and Supplementary Videos 1 and 2). Reintroduction of *B2M* in the B2M-deficient HCT-15 and LoVo cells diminished their killing by PD-1<sup>+</sup>  $\gamma\delta$  T cells (Vδ1 or Vδ3<sup>+</sup>) cells (Extended Data Fig. 6), suggesting that B2M loss increases the sensitivity to  $\gamma\delta$  T cells.

Next, we established two parental patient-derived tumour organoid lines (PDTOs; Supplementary Table 5) of MMR-d CRC and generated isogenic B2M<sup>KO</sup> lines using CRISPR. Genomic knockout of *B2M*



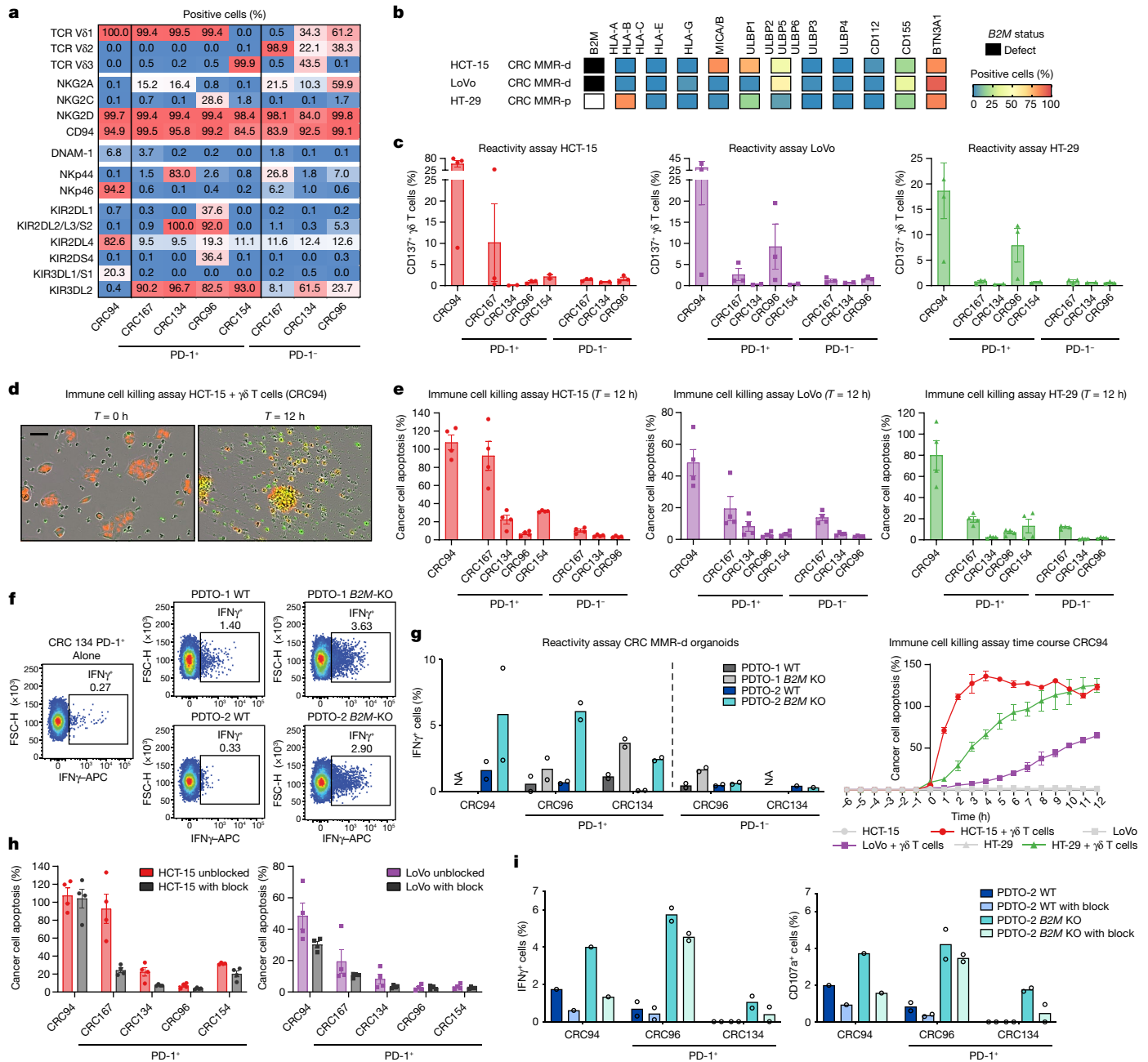


**Fig. 3** |  $\gamma\delta$  T cells from MMR-d colon cancers show preferential reactivity to HLA-class-I-negative cancer cell lines and organoids. **a**, The percentage of positive cells for the indicated markers on expanded  $\gamma\delta$  T cells from MMR-d colon cancers ( $n = 5$ ). **b**, Diagram showing the  $B2M$  status and surface expression of HLA class I, NKG2D ligands, DNAM-1 ligands and butyrophilin on CRC cell lines. MMR-p, MMR-proficient. **c**, CD137 expression on  $\gamma\delta$  T cells after co-culture with CRC cell lines. Data are mean  $\pm$  s.e.m. from at least two independent experiments. **d**, Representative images showing the killing of NuLightRed-transduced HCT-15 cells by  $\gamma\delta$  T cells in the presence of a green fluorescent caspase-3/7 reagent. Cancer cell apoptosis is visualized in yellow. Scale bar, 50  $\mu$ m. **e**, Quantification of the killing of CRC cell lines after co-culture with  $\gamma\delta$  T cells as described in **d**. Data are mean  $\pm$  s.e.m. of two wells with two images per well. A representative time course of cancer cell apoptosis is shown

at the bottom right. **f**, Representative flow cytometry plots showing IFN $\gamma$  expression in  $\gamma\delta$  T cells unstimulated (alone) and after stimulation with two  $B2M^{WT}$  and  $B2M^{KO}$  CRC MMR-d organoids. **g**, IFN $\gamma$  expression in  $\gamma\delta$  T cells after stimulation with two  $B2M^{WT}$  and  $B2M^{KO}$  CRC MMR-d organoids, shown as the difference compared with the unstimulated  $\gamma\delta$  T cell sample. Data are from two biological replicates, except for a single biological replicate of CRC134 PD-1<sup>-</sup>. NA, not available. **h**, The killing of CRC cell lines after 12 h co-culture with  $\gamma\delta$  T cells with or without NKG2D ligand blocking. Data are mean  $\pm$  s.e.m. of two wells with two images per well. **i**, IFN $\gamma$  (left) and CD107a (right) expression in  $\gamma\delta$  T cells after stimulation with  $B2M^{WT}$  PDTO-2 or  $B2M^{KO}$  PDTO-2, with or without NKG2D ligand blocking and subtracted background signal. Data are from two biological replicates, except for a single biological replicate of CRC94.

effectively abrogated cell surface expression of HLA class I (Extended Data Fig. 7). We exposed two  $B2M^{KO}$  lines and their parental  $B2M^{WT}$  lines to the expanded  $\gamma\delta$  T cell subsets, and quantified  $\gamma\delta$  T cell activation by determination of IFN $\gamma$  expression. Similar to our cell line data,  $\gamma\delta$  T cells displayed increased reactivity to  $B2M^{KO}$  PDTOs in comparison

to the  $B2M^{WT}$  PDTOs (Fig. 3f,g). Furthermore,  $\gamma\delta$  T cell reactivity to  $B2M^{KO}$  tumour organoids was preferentially contained within the PD-1<sup>+</sup> population of  $\gamma\delta$  T cells (Fig. 3g). Thus, a lack of HLA class I antigen presentation in MMR-d tumour cells can be effectively sensed by  $\gamma\delta$  T cells and stimulates their antitumour response.

Expression of NKG2D on  $\gamma\delta$  T cells decreased during co-culture with target cells (Extended Data Fig. 8a,b), suggesting the involvement of the NKG2D receptor in  $\gamma\delta$  T cell activity. The NKG2D ligands MICA/B and ULBPs were expressed by the cancer cell lines (Fig. 3b) and the MMR-d CRC PDOs, irrespective of their *B2M* status (Extended Data Fig. 7). To examine which receptor–ligand interactions might regulate the activity of PD-1<sup>+</sup>  $\gamma\delta$  T cells, we performed blocking experiments focused on (1) NKG2D, (2) DNAM-1 and (3)  $\gamma\delta$  TCR signalling. Of these candidates, the only consistent inhibitory effect was observed for NKG2D ligand blocking on cancer cells, which decreased the activation and killing ability of most PD-1<sup>+</sup>  $\gamma\delta$  T cells (Fig. 3h and Extended Data Fig. 8c,d), confirming the mechanistic involvement of the NKG2D receptor in  $\gamma\delta$  T cell activation in this context. Moreover, blocking NKG2D ligands on MMR-d CRC PDOs reduced the PDO-directed tumour reactivity of  $\gamma\delta$  T cells from CRC94 and CRC134 (Fig. 3i). Together, these results show that  $\gamma\delta$  T cell reactivity to MMR-d tumours is partly dependent on NKG2D/NKG2D-ligand interactions.

### ICB boosts V $\delta$ 1 and V $\delta$ 3 T cells in *B2M*<sup>MUT</sup> CRC

We subsequently studied how ICB influences  $\gamma\delta$  T cell infiltration and activation in MMR-d colon cancers in the therapeutic context. For this purpose, we analysed pre- and post-treatment samples of the NICHE trial<sup>9</sup>, in which patients with colon cancer were treated with neoadjuvant PD-1 plus CTLA-4 blockade. Consistent with our observations in the DRUP cohort, 4 out of 5 (80%) individuals with *B2M*<sup>MUT</sup> cancers in the NICHE trial showed a complete pathologic clinical response. Immunohistochemical analysis confirmed the loss of B2M protein expression on tumour cells in all mutated cases (Extended Data Fig. 9). Whereas expression of immune marker gene sets in the pretreatment samples was similar between 5 *B2M*<sup>MUT</sup> versus 13 *B2M*<sup>WT</sup> cancers, ICB induced a clear immunological divergence between these two groups (Fig. 4a). The *B2M*<sup>MUT</sup> subgroup was most significantly associated with higher post-treatment expression of *TRDV1* and *TRDV3* (two-sided Wilcoxon rank-sum test,  $P = 0.0067$ ; Fig. 4a), followed by higher expression of the general immune cell marker CD45, NK-cell-related markers, KIRs and  $\alpha\beta$ TCRs (two-sided Wilcoxon rank-sum test,  $P = 0.016$ ,  $P = 0.016$ ,  $P = 0.027$  and  $P = 0.043$ , respectively; Fig. 4a and Extended Data Fig. 10a). The set of KIRs upregulated after ICB in *B2M*<sup>MUT</sup> cancers (Extended Data Fig. 10b) was consistent with the sets of KIRs upregulated in *B2M*<sup>MUT</sup> MMR-d cancers in TCGA (Fig. 1e), and those expressed by MMR-d tumour-infiltrating  $\gamma\delta$  T cells (Fig. 2c). Pre- and post-ICB gene expression levels related to CD4 and CD8 infiltration were not associated with *B2M* status (Fig. 4a and Extended Data Fig. 10a).

To quantify and investigate the differences in immune profiles after ICB treatment, we used IMC to analyse tissues derived from five *B2M*<sup>MUT</sup> HLA-class-I-negative and five *B2M*<sup>WT</sup> HLA-class-I-positive cancers before and after ICB treatment. In the ICB-naive setting, *B2M*<sup>MUT</sup> MMR-d colon cancers showed higher  $\gamma\delta$  T cell infiltration compared with *B2M*<sup>WT</sup> MMR-d colon cancers (two-sided Wilcoxon rank-sum test,  $P = 0.032$ ; Fig. 4b and Extended Data Fig. 10c). Importantly, a large proportion of these  $\gamma\delta$  T cells showed an intraepithelial localization in *B2M*<sup>MUT</sup> MMR-d colon cancers compared with the *B2M*<sup>WT</sup> samples (two-sided Wilcoxon rank-sum test,  $P = 0.0079$ ; Extended Data Fig. 10d). No significant differences were observed in the infiltration of other immune cells, such as NK cells, CD4<sup>+</sup> T cells and CD8<sup>+</sup> T cells, in ICB-naive *B2M*<sup>MUT</sup> versus *B2M*<sup>WT</sup> MMR-d colon cancers (Fig. 4b). ICB treatment resulted in major pathologic clinical responses, and residual cancer cells were absent in most post-ICB samples. All post-ICB tissues showed a profound infiltration of different types of immune cells (Extended Data Fig. 10e), of which  $\gamma\delta$  T cells were the only immune subset that was significantly higher in ICB-treated *B2M*<sup>MUT</sup> compared with *B2M*<sup>WT</sup> MMR-d colon cancers (two-sided Wilcoxon rank-sum test,  $P = 0.016$ ; Fig. 4b and Extended Data Fig. 10c). In the sole *B2M*<sup>MUT</sup> case that still contained cancer cells after treatment with ICB, the majority of granzyme B<sup>+</sup>

immune cells infiltrating the tumour epithelium were  $\gamma\delta$  T cells (Fig. 4c). These  $\gamma\delta$  T cells displayed co-expression of CD103, CD39, Ki-67 and PD-1 (Extended Data Fig. 10f–h). Taken together, these results show that ICB treatment of MMR-d colon cancer increases the presence of activated, cytotoxic and proliferating  $\gamma\delta$  T cells at the tumour site, especially when these cancers are *B2M*-deficient, highlighting  $\gamma\delta$  T cells as effectors of ICB treatment within this context.

### Discussion

CD8<sup>+</sup>  $\alpha\beta$  T cells are major effectors of ICB<sup>11,12,27</sup> and rely on HLA class I antigen presentation of target cells. We confirm and shed light on the paradox that patients with HLA class I defects in MMR-d cancers retain the clinical benefit of ICB, suggesting that other immune effector cells are involved in compensating for the lack of conventional CD8<sup>+</sup> T cell immunity in this setting. We show that genomic inactivation of *B2M* in MMR-d colon cancers was associated with: (1) an elevated frequency of activated  $\gamma\delta$  T cells in ICB-naive tumours; (2) an increased presence of tumour-infiltrating  $\gamma\delta$  T cells after ICB treatment; (3) in vitro activation of tumour-infiltrating  $\gamma\delta$  T cells by CRC cell lines and PDOs; and (4) killing of tumour cell lines by  $\gamma\delta$  T cells, in particular by V $\delta$ 1 and V $\delta$ 3 subsets expressing PD-1.

Different subsets of  $\gamma\delta$  T cells exhibit substantially diverse functions that, in the context of cancer, range from tumour-promoting to tumour-icidal effects<sup>20,28,29</sup>. Thus, it is of interest to determine what defines antitumour reactivity of  $\gamma\delta$  T cells. Here we isolated V $\delta$ 1/3-expressing PD-1<sup>+</sup> T cells as well as V $\delta$ 2-expressing PD-1<sup>-</sup> T cells from MMR-d tumour tissues. Our data suggest that especially tumour-infiltrating V $\delta$ 1 and V $\delta$ 3 T cells can recognize and kill HLA-class-I-negative MMR-d tumours, whereas V $\gamma$ 9V $\delta$ 2 cells, the most studied and main subset of  $\gamma\delta$  T cells in the blood, appear to be less relevant within this context. This is consistent with other studies showing that the cytotoxic ability of V $\delta$ 1 cells generally outperforms their V $\delta$ 2 counterparts<sup>30–34</sup>. Notably, reports of the cytotoxicity of tumour-infiltrating V $\delta$ 3 cells have been lacking. Furthermore, the observation that PD-1<sup>+</sup>  $\gamma\delta$  T cells (V $\delta$ 1 and V $\delta$ 3 phenotype) demonstrated clearly higher levels of antitumour reactivity compared with their PD-1<sup>-</sup> counterparts (V $\delta$ 2 phenotype) suggests that, as for CD8<sup>+</sup>  $\alpha\beta$  T cells<sup>35</sup>, PD-1 expression may be a marker of antitumour reactivity in  $\gamma\delta$  T cells.

The mechanisms of activation of  $\gamma\delta$  T cells are notoriously complex and diverse<sup>20</sup>. Specifically, for V $\delta$ 1<sup>+</sup> cells, NKG2D has been described to be involved in tumour recognition, which is dependent on tumour cell expression of NKG2D ligands MICA/B and ULBPs<sup>36–38</sup>. Here, MICA/B and ULBPs were highly expressed by the MMR-d CRC cell lines and tumour organoids, and blocking these ligands reduced  $\gamma\delta$  T cell activation and cytotoxicity. This suggests a role for the activating receptor NKG2D in  $\gamma\delta$  T cell immunity to MMR-d tumours. Future research should address the outstanding question of how  $\gamma\delta$  T cells accumulate in *B2M*-deficient tumours, and whether the lack of CD8<sup>+</sup> T cell activity might contribute to the establishment of an attractive niche for  $\gamma\delta$  T cells and other immune effector cells. Potential mechanisms for the recognition of HLA-class-I-negative phenotypes may include KIR-, NKG2A- and LILRB1-mediated interactions with target cancer cells. Notably, we found that the expression of KIRs was most pronounced on PD-1<sup>+</sup>  $\gamma\delta$  T cells (V $\delta$ 1 or V $\delta$ 3<sup>+</sup> subsets), which demonstrated anti-tumour activity. Whether the lack of KIR-mediated signalling promotes the survival of  $\gamma\delta$  T cells and their intratumoural proliferation remains to be studied.

Our findings have broad implications for cancer immunotherapy. First, our findings strengthen the rationale for combining PD-1 blockade with immunotherapeutic approaches to further enhance  $\gamma\delta$  T-cell-based antitumour immunity. Second, the presence or absence in tumours of specific  $\gamma\delta$  T cell subsets (such as V $\delta$ 1 or V $\delta$ 3) may help to define patients who are responsive or unresponsive to ICB, respectively, especially in the case of MMR-d cancers and

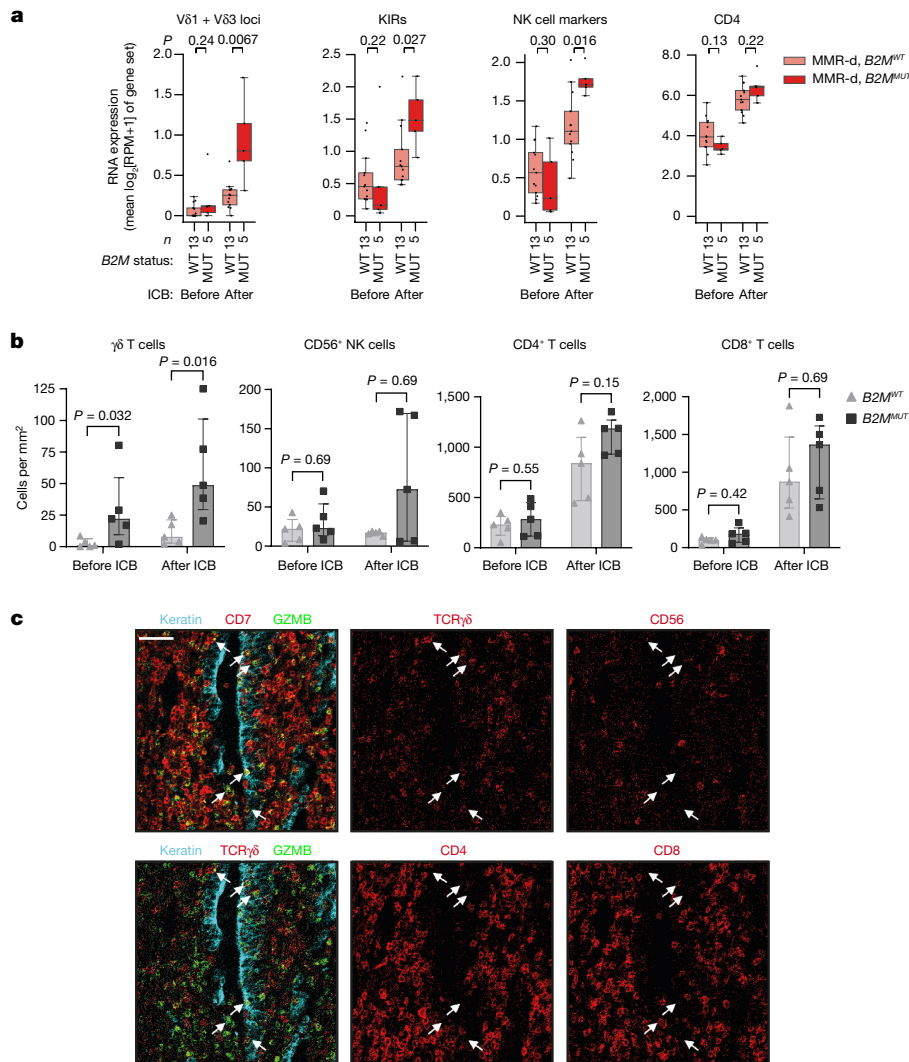


**Fig. 4 | ICB induces substantial infiltration of  $\gamma\delta$  T cells into MMR-d colon cancers with defects in antigen presentation.** **a**, The RNA expression of different immune marker gene sets in MMR-d  $B2M^{WT}$  (pink) and MMR-d  $B2M^{MUT}$  (red) cancers before (left) and after (right) neoadjuvant ICB in the NICHE study. The boxes, whiskers and dots indicate quartiles,  $1.5 \times$  IQR and individual data points, respectively.  $P$  values were calculated using two-sided Wilcoxon rank-sum tests comparing MMR-d  $B2M^{WT}$  versus MMR-d  $B2M^{MUT}$  cancers. **b**, The

frequencies of  $\gamma\delta$  T cells, CD56<sup>+</sup> NK cells, CD4<sup>+</sup> T cells and CD8<sup>+</sup> T cells in  $B2M^{WT}$  ( $n = 5$ ) and  $B2M^{MUT}$  ( $n = 5$ ) MMR-d colon cancers before and after ICB treatment. Data are median  $\pm$  IQR, with individual samples (dots).  $P$  values were calculated using two-sided Wilcoxon rank-sum tests. **c**, Representative images of granzyme-B-positive  $\gamma\delta$  T cells infiltrating the tumour epithelium (white arrows) by IMC analysis of a  $B2M^{MUT}$  MMR-d colon cancer after ICB treatment. Scale bar, 50  $\mu$ m.

other malignancies with frequent HLA class I defects, such as stomach adenocarcinoma<sup>39</sup> and Hodgkin's lymphoma<sup>40</sup>. Third, our results suggest that MMR-d cancers and other tumours with HLA class I defects may be particularly attractive targets for V $\delta$ 1 or V $\delta$ 3 T-cell-based cellular therapies.

Although we have provided detailed and multidimensional analyses, it is probable that  $\gamma\delta$  T cells are not the only factor driving ICB responses in HLA-class-I-negative MMR-d CRC tumours. In this context, other HLA-class-I-independent immune subsets, such as NK cells and neoantigen-specific CD4<sup>+</sup> T cells may also contribute. The latter were shown to have an important role in the response to ICB (as reported in mouse  $B2M$ -deficient MMR-d cancer models<sup>41</sup>), and may also support  $\gamma\delta$  T-cell-driven responses. Notably, no subset equivalent to V $\delta$ 1 or V $\delta$ 3 T cells has been identified in mice, which complicates their investigation in *in vivo* models. In conclusion, our results provide strong evidence that  $\gamma\delta$  T cells are cytotoxic effector cells of ICB treatment in HLA-class-I-negative MMR-d colon cancers, with implications for further exploitation of  $\gamma\delta$  T cells in cancer immunotherapy.

## Online content

Any methods, additional references, Nature Portfolio reporting summaries, source data, extended data, supplementary information, acknowledgements, peer review information; details of author contributions and competing interests; and statements of data and code availability are available at <https://doi.org/10.1038/s41586-022-05593-1>.

1. Ionov, Y., Peinado, M. A., Malkhosyan, S., Shibata, D. & Perucho, M. Ubiquitous somatic mutations in simple repeated sequences reveal a new mechanism for colonic carcinogenesis. *Nature* **363**, 558–561 (1993).
2. Germano, G. et al. Inactivation of DNA repair triggers neoantigen generation and impairs tumour growth. *Nature* **552**, 116–120 (2017).
3. Zaretsky, J. M. et al. Mutations associated with acquired resistance to PD-1 blockade in melanoma. *N. Engl. J. Med.* **375**, 819–829 (2016).
4. Gettinger, S. et al. Impaired HLA class I antigen processing and presentation as a mechanism of acquired resistance to immune checkpoint inhibitors in lung cancer. *Cancer Discov.* **7**, 1420–1435 (2017).
5. Sade-Feldman, M. et al. Resistance to checkpoint blockade therapy through inactivation of antigen presentation. *Nat. Commun.* **8**, 1136 (2017).
6. Le, D. T. et al. Mismatch repair deficiency predicts response of solid tumors to PD-1 blockade. *Science* **357**, 409–413 (2017).



7. Overman, M. J. et al. Nivolumab in patients with metastatic DNA mismatch repair-deficient or microsatellite instability-high colorectal cancer (CheckMate 142): an open-label, multicentre, phase 2 study. *Lancet. Oncol.* **18**, 1182–1191 (2017).
8. Overman, M. J. et al. Durable clinical benefit with nivolumab plus ipilimumab in DNA mismatch repair-deficient/microsatellite instability-high metastatic colorectal cancer. *J. Clin. Oncol.* **36**, 773–779 (2018).
9. Chalabi, M. et al. Neoadjuvant immunotherapy leads to pathological responses in MMR-proficient and MMR-deficient early-stage colon cancers. *Nat. Med.* **26**, 566–576 (2020).
10. Dolcetti, R. et al. High prevalence of activated intraepithelial cytotoxic T lymphocytes and increased neoplastic cell apoptosis in colorectal carcinomas with microsatellite instability. *Am. J. Pathol.* **154**, 1805–1813 (1999).
11. Tumeah, P. C. et al. PD-1 blockade induces responses by inhibiting adaptive immune resistance. *Nature* **515**, 568–571 (2014).
12. Taube, J. M. et al. Association of PD-1, PD-1 ligands, and other features of the tumor immune microenvironment with response to anti-PD-1 therapy. *Clin. Cancer Res.* **20**, 5064–5074 (2014).
13. Bicknell, D. C., Kaklamanis, L., Hampson, R., Bodmer, W. F. & Karran, P. Selection for  $\beta_2$ -microglobulin mutation in mismatch repair-defective colorectal carcinomas. *Curr. Biol.* **6**, 1695–1697 (1996).
14. Kloor, M. et al. Immunoselective pressure and human leukocyte antigen class I antigen machinery defects in microsatellite unstable colorectal cancers. *Cancer Res.* **65**, 6418–6424 (2005).
15. Dierssen, J. W. et al. HNPCC versus sporadic microsatellite-unstable colon cancers follow different routes toward loss of HLA class I expression. *BMC Cancer* **7**, 33 (2007).
16. Ijsselstein, M. E. et al. Revisiting immune escape in colorectal cancer in the era of immunotherapy. *Br. J. Cancer* **120**, 815–818 (2019).
17. Hughes, E. A., Hammond, C. & Cresswell, P. Misfolded major histocompatibility complex class I heavy chains are translocated into the cytoplasm and degraded by the proteasome. *Proc. Natl Acad. Sci. USA* **94**, 1896–1901 (1997).
18. Middha, S. et al. Majority of B2M-mutant and -deficient colorectal carcinomas achieve clinical benefit from immune checkpoint inhibitor therapy and are microsatellite instability-high. *JCO Precis. Oncol.* **3**, 1–14 (2019).
19. Groh, V. et al. Human lymphocytes bearing T cell receptor  $\gamma/\delta$  are phenotypically diverse and evenly distributed throughout the lymphoid system. *J. Exp. Med.* **169**, 1277–1294 (1989).
20. Silva-Santos, B., Mensurado, S. & Coffelt, S. B.  $\gamma\delta$  T cells: pleiotropic immune effectors with therapeutic potential in cancer. *Nat. Rev. Cancer* **19**, 392–404 (2019).
21. Halary, F. et al. Control of self-reactive cytotoxic T lymphocytes expressing  $\gamma\delta$  T cell receptors by natural killer inhibitory receptors. *Eur. J. Immunol.* **27**, 2812–2821 (1997).
22. de Vries, N. L. et al. High-dimensional cytometric analysis of colorectal cancer reveals novel mediators of antitumour immunity. *Gut* **69**, 691–703 (2020).
23. van der Velden, D. L. et al. The Drug Rediscovery protocol facilitates the expanded use of existing anticancer drugs. *Nature* **574**, 127–131 (2019).
24. Danaher, P. et al. Gene expression markers of tumor infiltrating leukocytes. *J. Immunother. Cancer* **5**, 18 (2017).
25. Priestley, P. et al. Pan-cancer whole-genome analyses of metastatic solid tumours. *Nature* **575**, 210–216 (2019).
26. Duhon, T. et al. Co-expression of CD39 and CD103 identifies tumor-reactive CD8 T cells in human solid tumors. *Nat. Commun.* **9**, 2724 (2018).
27. Kwon, M. et al. Determinants of response and intrinsic resistance to PD-1 blockade in microsatellite instability-high gastric cancer. *Cancer Discov.* **11**, 2168–2185 (2021).
28. Wu, Y. et al. An innate-like V $\delta$ 1<sup>+</sup>  $\gamma\delta$  T cell compartment in the human breast is associated with remission in triple-negative breast cancer. *Sci. Transl. Med.* **11**, eaax9364 (2019).
29. Wu, Y. et al. A local human V $\delta$ 1 T cell population is associated with survival in nonsmall-cell lung cancer. *Nat. Cancer* **3**, 696–709 (2022).
30. Mæurer, M. J. et al. Human intestinal V $\delta$ 1<sup>+</sup> lymphocytes recognize tumor cells of epithelial origin. *J. Exp. Med.* **183**, 1681–1696 (1996).
31. Siegers, G. M., Ribot, E. J., Keating, A. & Foster, P. J. Extensive expansion of primary human gamma delta T cells generates cytotoxic effector memory cells that can be labeled with feraheme for cellular MRI. *Cancer Immunol. Immunother.* **62**, 571–583 (2013).
32. Wu, D. et al. Ex vivo expanded human circulating V $\delta$ 1  $\gamma\delta$  T cells exhibit favorable therapeutic potential for colon cancer. *Oncoimmunology* **4**, e992749 (2015).
33. Almeida, A. R. et al. Delta one T cells for immunotherapy of chronic lymphocytic leukemia: clinical-grade expansion/differentiation and preclinical proof of concept. *Clin. Cancer Res.* **22**, 5795–5804 (2016).
34. Mikulak, J. et al. NKp46-expressing human gut-resident intraepithelial V $\delta$ 1 T cell subpopulation exhibits high antitumor activity against colorectal cancer. *JCI Insight* **4**, e125884 (2019).
35. van der Leun, A. M., Thommen, D. S. & Schumacher, T. N. CD8<sup>+</sup> T cell states in human cancer: insights from single-cell analysis. *Nat. Rev. Cancer* **20**, 218–232 (2020).
36. Groh, V., Steinle, A., Bauer, S. & Spies, T. Recognition of stress-induced MHC molecules by intestinal epithelial  $\gamma\delta$  T cells. *Science* **279**, 1737–1740 (1998).
37. Groh, V. et al. Broad tumor-associated expression and recognition by tumor-derived  $\gamma\delta$  T cells of MICA and MICB. *Proc. Natl Acad. Sci. USA* **96**, 6879–6884 (1999).
38. Poggi, A. et al. V $\delta$ 1 T lymphocytes from B-CLL patients recognize ULBP3 expressed on leukemic B cells and up-regulated by *trans*-retinoic acid. *Cancer Res.* **64**, 9172–9179 (2004).
39. Hause, R. J., Pritchard, C. C., Shendure, J. & Salipante, S. J. Classification and characterization of microsatellite instability across 18 cancer types. *Nat. Med.* **22**, 1342–1350 (2016).
40. Cader, F. Z. et al. A peripheral immune signature of responsiveness to PD-1 blockade in patients with classical Hodgkin lymphoma. *Nat. Med.* **26**, 1468–1479 (2020).
41. Germano, G. et al. CD4 T cell-dependent rejection of beta-2 microglobulin null mismatch repair-deficient tumors. *Cancer Discov.* **11**, 1844–1859 (2021).

**Publisher's note** Springer Nature remains neutral with regard to jurisdictional claims in published maps and institutional affiliations.



**Open Access** This article is licensed under a Creative Commons Attribution 4.0 International License, which permits use, sharing, adaptation, distribution and reproduction in any medium or format, as long as you give appropriate credit to the original author(s) and the source, provide a link to the Creative Commons licence, and indicate if changes were made. The images or other third party material in this article are included in the article's Creative Commons licence, unless indicated otherwise in a credit line to the material. If material is not included in the article's Creative Commons licence and your intended use is not permitted by statutory regulation or exceeds the permitted use, you will need to obtain permission directly from the copyright holder. To view a copy of this licence, visit <http://creativecommons.org/licenses/by/4.0/>.

© The Author(s) 2023